



OPEN ACCESS

EDITED BY

Barry Alan Gardiner,
Institut Européen De La Forêt Cultivée (IEFC),
France

REVIEWED BY

Wenjie Wang,
Zhejiang Agriculture and Forestry University,
China
Victor L. Barradas,
National Autonomous University of Mexico,
Mexico

*CORRESPONDENCE

Kun Xu
✉ kunxu1@hbnu.edu.cn

RECEIVED 26 February 2024

ACCEPTED 03 October 2024

PUBLISHED 15 October 2024

CITATION

Liu Y, Zhang J, Rao S and Xu K (2024) Sleet damage to branches and crowns of street camphor trees (*Cinnamomum camphora*) in a central China mega-city: damage statistics, modelling, and implications.
Front. For. Glob. Change 7:1391645.
doi: 10.3389/ffgc.2024.1391645

COPYRIGHT

© 2024 Liu, Zhang, Rao and Xu. This is an open-access article distributed under the terms of the [Creative Commons Attribution License \(CC BY\)](https://creativecommons.org/licenses/by/4.0/). The use, distribution or reproduction in other forums is permitted, provided the original author(s) and the copyright owner(s) are credited and that the original publication in this journal is cited, in accordance with accepted academic practice. No use, distribution or reproduction is permitted which does not comply with these terms.

Sleet damage to branches and crowns of street camphor trees (*Cinnamomum camphora*) in a central China mega-city: damage statistics, modelling, and implications

Yichen Liu, Junru Zhang, Shanshan Rao and Kun Xu*

College of Life Sciences, Hubei Normal University, Huangshi, China

Introduction: Extreme weather becomes increasingly frequent and severe under climate change, causing unexpected damage to trees. Among them, sleet damage is particularly harmful to evergreen trees in subtropical area. Camphor trees (*Cinnamomum camphora*), as dominant street trees in central China, are prone to sleet damage, resulting in loss of valuable ecosystem functions.

Methods: By measuring tree size characteristics of 118 camphor trees before and after a record-breaking sleet event in Wuhan, a mega-city in central China, we built allometric equations between size and volume of broken branches and used the random forest regression to model sleet damage to camphor trees.

Results: We identified that larger trees with intermediate bole height suffered more than smaller trees with tall bole height from the sleet event. We estimated the volume of broken branches of a camphor tree with DBH at 35.0 cm as 106.4 dm³, equivalent to 55.3 kg biomass loss, from the sleet event.

Discussion: We suggest that pruning the branches instead of topping the main stems of small camphor trees would reduce the sleet hazard. To mitigate the negative impacts of climate change, regular pruning should be practiced on street camphor trees to protect them from future heavy sleet events.

KEYWORDS

sleet, extreme weather, broken branch, *Cinnamomum camphora*, street tree, allometric equation, random forest regression, central China

1 Introduction

Sleet, like other recurring extreme weather events, will become more frequent and severe under climate change (Karl et al., 2008; Rummukainen, 2012; Ohba, 2021), challenging efforts on mitigating the negative ecological consequences of these events (Maxwell et al., 2019). Unlike typical precipitation such as rainfall, snow and hail, sleet forms when snowflakes partially melt and fall through a shallow layer of warm air, known as the inversion layer (Livanov, 2023). Particularly in sleet, the ice surface on leaves and fruits of trees accumulates, adding weight to twigs and branches (Proulx and Greene, 2001; Ohba, 2021). When iced leaves and fruits become too heavy to support, twigs and branches break (Burke et al., 1976; Campos et al., 2023). Damage by sleet and other extreme cold weather events on trees and forest ecosystems can be large (Downton and Miller, 1993; Turcotte et al., 2012; Wang et al., 2016; Zhao et al., 2020; Gao et al., 2024), e.g., one-third of Florida's commercial citrus trees died in the 1980s' extreme cold spells (Downton and Miller, 1993) and 10% of total forests in southern China damaged in

the 2008 ice storm (Gao et al., 2024). Sleet damage is more severe on evergreen trees than deciduous trees not only because the formers' leaves become tougher and crowns become heavier in sleet (Proulx and Greene, 2001; Turcotte et al., 2012; Niinemets, 2016), but also because the formers' woods and barks are brittle and prone to break under external force (Hauer et al., 1993; McPherson et al., 2016b; Matsushita et al., 2020). It is even harsher to broadleaf evergreen trees because their leaf area is larger, favoring formation of a larger ice surface (Proulx and Greene, 2001; Turcotte et al., 2012; Levia et al., 2017). Severe sleet has been rare in subtropical monsoon climates (Zhao et al., 2020), but recently has occurred more frequently, e.g., in 2008, 2018, and 2024 (Wang et al., 2016; Zhao et al., 2020; Weather Station of Wuhan, 2024). The increasing frequency and severity of sleet is expected to increase damage to broadleaf evergreen trees in the subtropical monsoon climate zone, e.g., in southern and central China (Wang et al., 2016; Yan and Yang, 2018; Zhao et al., 2020).

Urban forests and street trees are essential green infrastructure providing various ecosystem functions, such as carbon sink, air purification, biodiversity support, and food and medicine sources (McPherson et al., 2016a; Zhou and Yan, 2016; Chen et al., 2020). Street trees provide over half of the global population living in cities with shade, environmental amelioration, and recreation (Wu, 2019), which are crucial for sustaining the urban ecosystem (Gómez et al., 2011). Among important street tree species, camphor trees (*Cinnamomum camphora*) are a common broadleaf evergreen tree species widely distributing in eastern Asia, especially central China (Wu et al., 2020; Liang et al., 2024; Zhang et al., 2024), and planted in three other continents (Wood and Esaian, 2020; Xiang et al., 2020). A key ecological role of camphor trees for sustaining urban habitats is to support bird diversity with large and dense closed crowns (Wood and Esaian, 2020) and black round fruit (Wood and Esaian, 2020; Xiao et al., 2023), a preferred food source for urban birds (Chupp and Battaglia, 2016). Camphor trees are also valuable sources of timber, medicine, pesticide, and ornaments for urban areas in China (Zhou and Yan, 2016; Chen et al., 2020). As a native tree species, they are primary street trees in over 20 provinces of China (Xiang et al., 2020), and are the most abundant street trees in 12 major cities of China, including the mega-city Wuhan (also the capital of Hubei Province) (Liu and Slik, 2022; Liang et al., 2024). With an aim to quickly green up urban area and enhance urban ecosystem functions (Wang et al., 2018), over 100 thousand camphor trees were planted on streets in central China, especially in Hubei Province, providing important ecological functions for the urban ecosystem (Xiang et al., 2020; Liu and Slik, 2022; Zhang et al., 2024). A common management practice on street camphor trees is pruning the branches for shaping and promoting growth of stems (Velázquez-Martí et al., 2011; Speak and Salbitano, 2023). By regularly pruning the branches of street camphor trees, their stems can grow taller and horizontal branch spread can be reduced (Zhou and Yan, 2016; Speak and Salbitano, 2023).

Under climate change, camphor trees are expected to suffer increasing natural hazards to branches and crowns, especially those in populated urban area where street camphor trees dominate and they are exposed directly to strong wind, ice storm, heavy snow, and sleet (Hauer et al., 1993; Irland, 2000; Zhu et al., 2004; Yan and Yang, 2018; Xiang et al., 2020). After sleet, the weight of frozen ice added on branches and crowns of a camphor tree can reach over 10 times its dry weight (Hauer et al., 1993), resulting in damaged stems that need to regrow and open canopies that require years to refill (Wang et al., 2016). In cities, broken branches and crowns of street camphor trees

were collected and treated as residual waste by city cleaners, resulting in carbon source as loss of biomass equivalent to the dry weight of broken branches and crowns (Braghiroli and Passarini, 2020). Birds foraging camphor fruits would receive less support for food due to fruits damaged by sleet (Wood and Esaian, 2020). The most severe damage by sleet on camphor trees was mortality due to complete loss of branches (Zhao et al., 2020), which has been recorded in several cities across China (Yan and Yang, 2018), including Wuhan which experienced a record-breaking sleet event in February 2024 (Weather Station of Wuhan, 2024). Shorter bole and earlier branching form were found to be related to heavier ice storm damage to camphor trees (Chau et al., 2020). On the contrary, small camphor trees with few branches and small crowns were less affected by the extreme cold weather (Levia et al., 2017; Campos et al., 2023). These relations are expected as larger trees gain more weight from ice accumulated on leaves and barks than smaller trees according to the allometric relationship between tree size (i.e., diameter at breast height (DBH) and height) and volume (Mohler et al., 1978; White, 1981). Camphor trees, either naturally regenerated or planted, follow the allometries between tree size and volume of stems and crowns (Jucker et al., 2022; Bornand et al., 2023). However, no allometric relationship was identified between size and volume of branches damaged by sleet event. Also, no model has been established for sleet damage to street trees in central China, including camphor trees. Considering this, we assessed sleet damage to street camphor trees in Wuhan and attempted to answer if sleet damage to trees of larger DBH and height are exponentially more severe than that to smaller trees? We further modelled the relationship between tree size and sleet damage to branches and crowns of street camphor trees. Based on estimated models, we discussed whether pruning would be an effective way to reduce future heavy sleet damage to street camphor trees under climate change.

2 Materials and methods

2.1 Study area

Our study area is two intersecting 500-m streets within 30.64232° N, 114.32288° E–30.64498° N, 114.31701° E in Wuhan, China (Figure 1a). Camphor trees are the most abundant street trees in Wuhan (Liu and Slik, 2022), and the single dominant street tree species in our study area. The camphor trees in the study area were transplanted in 2008 when urbanization was completed, and received no pruning or other treatment since 2019. According to the characterization of street trees in Wuhan (Liang et al., 2024), DBH, height, bole height, and crown size of street camphor trees in our study area are within the 1st and 3rd quartiles of each characteristic.

Located in the subtropical monsoon climate zone, Wuhan's annual mean temperature is 16.9°C and annual precipitation is 1280.9 mm with most rainfall between April and October (Lv et al., 2011). A record-breaking sleet event began on the 2nd and ended on the 4th February 2024, bringing 42.8 mm precipitation (Weather Station of Wuhan, 2024). There was a sudden decrease in daily mean temperature from 9.0°C to −1.0°C (Figure 1b). Mean daily wind speed remained at around 5.0 m/s during this period, while daily mean temperature remained below 0°C for another 3 days after the sleet (Figure 1b). Ice surface accumulated on camphor leaves and fruits (Figure 2a), resulting in branches breaking from stems and falling on the ground (Figure 2b).

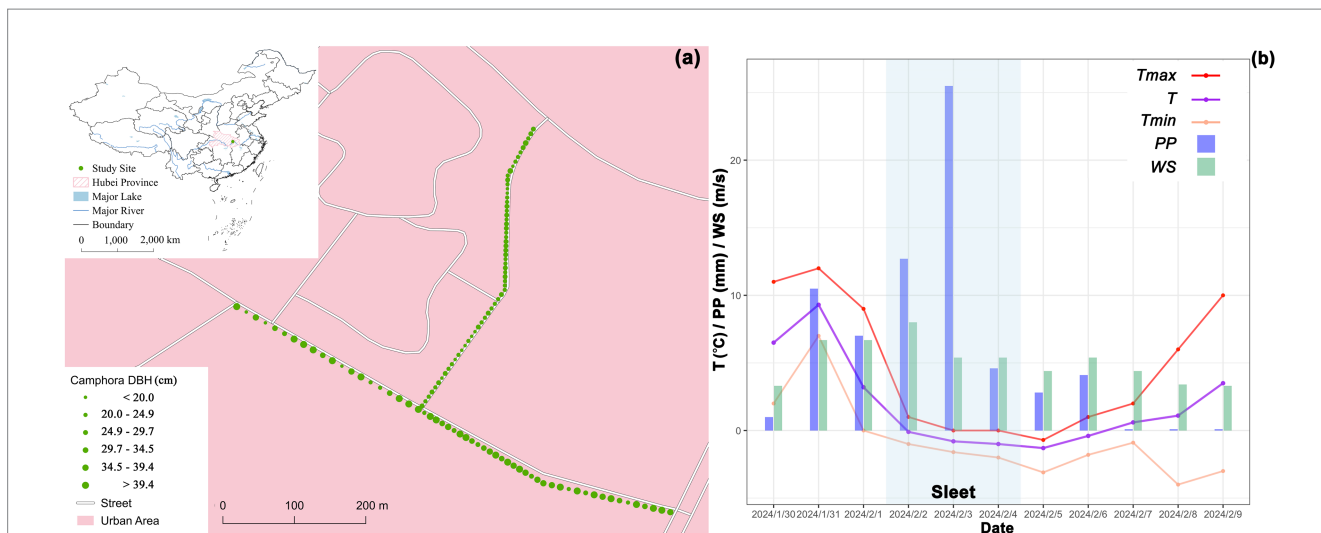


FIGURE 1 Locations of the 118 camphor trees measured and **(b)** Daily weather conditions in Wuhan, China for the period from the 30th January 2024 to the 9th February 2024. **(a)** Sizes of green dots represent tree DBH from below 20.0 to above 39.4 cm. **(b)** The sleet period from the 2nd to the 4th February 2024 is shown in light blue. PP, WS, and T represent daily precipitation (mm; blue bar), mean daily wind speed (m/s; green bar), and daily mean temperature ($^{\circ}$ C; purple solid line), respectively. Maximum and minimum hourly temperature for each day, as Tmax and Tmin, are shown by the red and orange dashed lines.

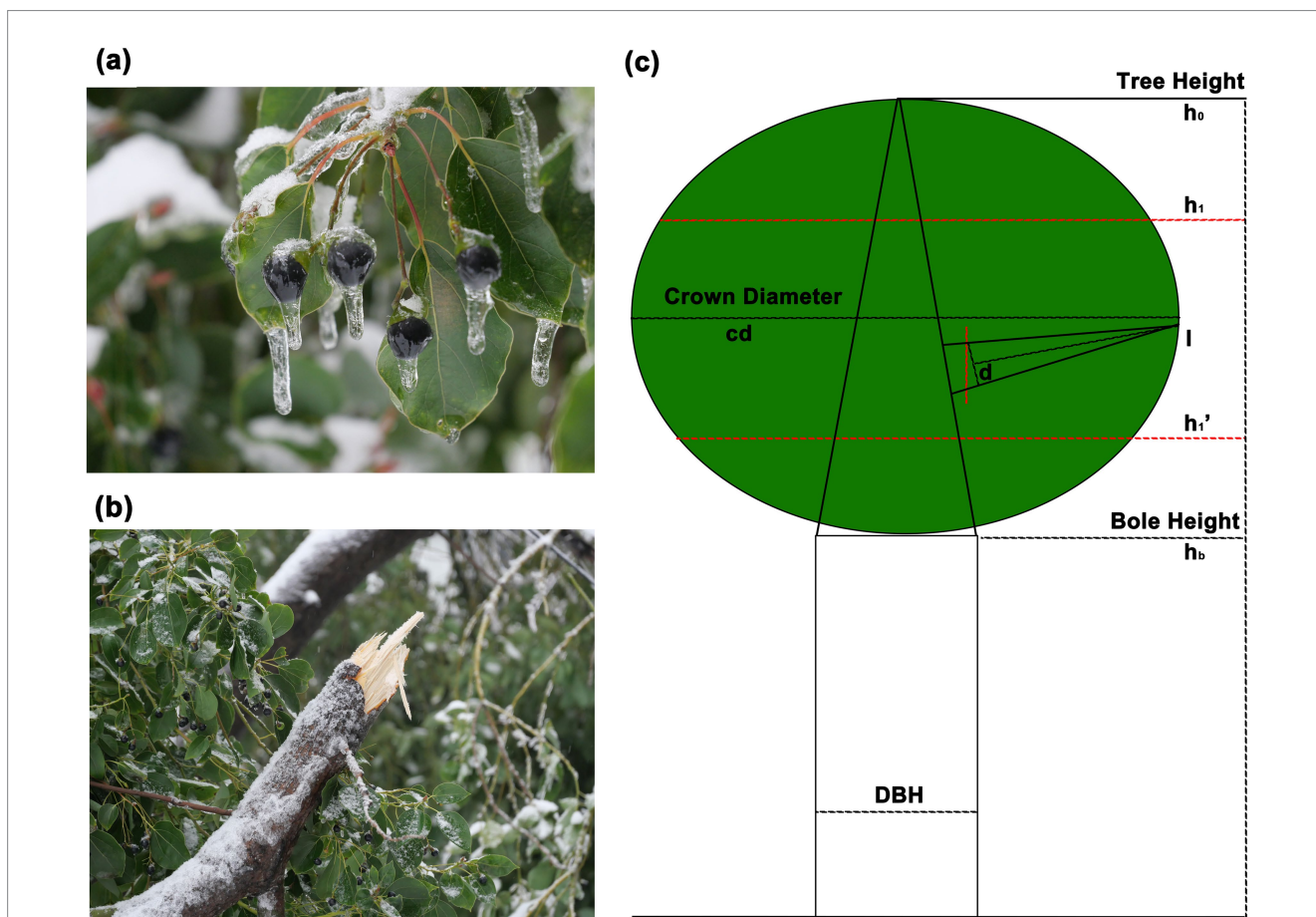


FIGURE 2 **(a)** Camphor fruits and leaves frozen by the sleet event. **(b)** A broken branch from a camphor tree after the sleet event. **(c)** Illustration of the tree measurements (DBH, h_0 , h_1 , h_b , and cd) taken in this study. **(a,b)** Taken on the 4th February 2024 by the corresponding author in the study area. **(c)** Red dashed lines indicate sleet damage to a branch (with measurements of the broken branch, d and l), and to the crown in two scenarios (h_1 and h_1' , where $h_0 \geq h_1 > (h_b + h_0)/2$ and $(h_b + h_0)/2 \geq h_1' > h_b$).

2.2 Tree measurements

We measured tree size characteristics of each of the 118 camphor trees along the two 500-m streets (Figure 2c) before and after the sleet event. Before the sleet (on the 30th and 31st January 2024), we measured diameter at breast height (DBH), height (h_0), bole height (h_b ; height of the lowest branching point on the main stem), crown diameter (cd); (major + minor axes of crown/2) of each tree. After the sleet (on the 8th and 9th February 2024), we remeasured each tree for its height (h_1), top status (ts; 0 for intact and 1 for broken top, respectively), and number of broken branches (on the main stem only) (n_b). We conducted a paired t test on tree height before and after the sleet (h_0 versus h_1).

For broken branches, we measured diameter (d), length (l), and number of twigs (n_t) of branches on the ground near each tree, and we determined the diameter class (dc) of other broken branches by signs of fresh cracks on the main stem. We used a clinometer and Bosch GLM 50–27 CG Professional Laser Distance Measurement Device (Stereńczak et al., 2019) to measure h_0 , h_1 , h_b and cd. DBH of each tree, and d and l of broken branches were measured using a diameter tape. We visually assessed ts, n_b , n_t , and classed dc by 1 cm increments from 1 to 18 cm. We counted the number of broken branches with fresh cracks from the top to the bottom of each tree to ensure that we recorded all branches with $d \geq 1.0$ cm damaged by the sleet event. After the field survey, we examined distribution of each measurement and Pearson's correlation coefficient between each pair using the R package PerformanceAnalytics (Carl et al., 2010).

2.3 Volume estimates

Stem volume before the sleet (vs_0) was approximated by a cylinder below bole height plus a cone above bole height (Jucker et al., 2022; Zhang et al., 2024) following:

$$vs_0 = \pi R^2 H + \frac{\pi r^2 h}{3}, \quad (1)$$

where $R=r=DBH/2$, $H=h_b$ and $h=h_0 - h_b$ (Figure 2c) (McPherson et al., 2016b).

Crown volume before the sleet (vc_0) was approximated by an ellipsoid following:

$$vc_0 = \frac{4\pi abc}{3}, \quad (2)$$

where $a=b=cd/2$ and $c=(h_0 - h_b)/2$ (Figure 2c) (Wang and Jarvis, 1990).

Volume of a broken branch (vbb) was approximated by a cone following:

$$vbb = \frac{\pi rb^2 l}{3}, \quad (3)$$

where $rb=d/2$ (Figure 2c) (McPherson et al., 2016a).

Then, we estimated stem volume after the sleet (vs_1) with a cylinder below bole height plus a truncated cone by deducting the volume of the upper cone (Figure 2c) following:

$$vs_1 = \pi \frac{DBH^2}{4} h_b + \frac{\pi DBH^2 [(h_0 - h_b)^3 - (h_0 - h_1)^3]}{12(h_0 - h_b)^2}. \quad (4)$$

And we estimated crown volume after the sleet (vc_1) with a truncated ellipsoid in two damage scenarios (Figure 2c) following:

$$vc_1 = \left(\frac{h_0 - h_b}{2} - \frac{2(h_0 - h_1)^3}{(h_0 - h_b)^2} \right) \times \frac{\pi cd^2}{3} \quad (5)$$

for $h_0 \geq h_1 > (h_b + h_0)/2$, and

$$vc_1 = \frac{2(h'_1 - h_b)^3}{(h_0 - h_b)^2} \times \frac{\pi cd^2}{3} \quad (6)$$

for $(h_b + h_0)/2 \geq h'_1 > h_b$.

2.4 Allometric equation

We estimated the allometric relationship between diameter (d) and volume (vbb) of broken branches tape measured following:

$$\ln(vbb) = a + b \cdot \ln(d) + \varepsilon, \quad (7)$$

where a and b are parameters and ε is the random error (Mohler et al., 1978; White, 1981). We then estimated the volume for each diameter class (dc) by substituting the midpoint of each interval of d in the parameterized Equation 7 using R 4.3.2 (R Core Team, 2023). We then calculated the total volume of broken branches of each tree (vbtt) by summing the estimated volume of each broken branch of the tree. We also examined the allometries between DBH and tree height (h_0) and between DBH and crown diameter (cd) using the R package PerformanceAnalytics (Carl et al., 2010).

2.5 Sleet damage assessment

We assessed sleet damage to camphor trees using top status (ts), total volume of broken branches (vbtt), loss of stem volume ($vs_b = vs_0 - vs_1$), loss of crown volume ($vc_b = vc_0 - vc_1$), and the ratio between the volume of broken branches and of the stem before the sleet ($rvbs = vbtt/vs_0$). Here, ts is a binary variable and the other four are continuous variables.

2.6 Random forest regression

We used the random forest regression with 500 trees and 1 variable at each split (Breiman, 2001) to model each type of sleet damage (i.e., ts, vbtt, vs_b , vc_b , and $rvbs$) with DBH, height before

the sleet (h_0), bole height (h_b), and crown diameter (cd) as regressors. The algorithm of random forest method handles multicollinearity and nonlinear effects for regression (Garg and Tai, 2013). Prediction accuracy of the random regression models was measured by error rate for classification and area under the receiver operating characteristic curve (AUC) for ts and by percentage of variation explained for vbbt, vs_b , vc_b , and $rvbs$ (Breiman, 2001). We did not use height after the sleet (h_1) of the tree as a regressor because we aimed to predict sleet damage.

The importance of variables of each random forest regression model was plotted, and was measured by the decrease of model accuracy by removing the variable from the model (Breiman, 2001). We created the partial dependence plots on individual regressors, i.e., DBH, h_0 , h_b , and cd, for each model using the R package pdp (Greenwell, 2017). We also created the partial dependence plots on combination between DBH and h_b for each model. Because h_0 and cd were correlated with DBH (Supplementary Figure S1a) and because they were less easy to measure, we did not produce partial dependence plots on combination between DBH and h_0 or cd.

Based on the random forest regression model for vbbt, we then estimated the loss of biomass from branches of a camphor tree of 35.0 cm DBH broken in the sleet by multiplying its estimated vbbt and the average dried weight of camphor woods, i.e., 0.52 kg/dm³ (Miles and Smith, 2009; McPherson et al., 2016b). We also examined the effects of DBH and h_b on vbbt using two-way ANOVA by grouping DBH in three classes (DBH < 27, 27 ≤ DBH < 40, and DBH ≥ 40 cm) and h_b in four classes (h_b < 4.5, 4.5 ≤ h_b < 5.5, 5.5 ≤ h_b < 6.5, and h_b ≥ 6.5 cm) with equal intervals. Multiple comparison was conducted for each level of DBH and h_b classes using the TukeyHSD function in R.

3 Results

3.1 Tree measurements

The DBH of the 118 camphor trees ranges from 14.8 to 57.7 cm with a mean of 29.8 cm and a standard deviation of 9.7 cm (Table 1; Supplementary Figure S1a). Height before (h_0) and after the sleet (h_1) of the 118 trees were 8.1–23.2 m and 6.3–18.2 m, respectively (Table 1; Supplementary Figure S1a), where h_1 was significantly smaller than h_0 by 4.3 m (paired *t* test *p*-value < 0.001). Bole height (h_b) ranged from 3.0 to 8.0 m, and crown diameter (cd) from 3.2 to 17.5 m (Table 1; Supplementary Figure S1a). Estimated volumes of stem and crown were 125.0–2893.7 dm³ and 19.84–2905.34 dm³, respectively (Equations 1–6; Supplementary Figure S1b).

In total, there were 761 broken branches identified from the 118 trees, and 170 branches were measured. The number of broken branches by the sleet event was 1–21 with a mean of 4.9 and a standard deviation of 3.4 (Table 1). Diameter and length of the 170 measured broken branches ranged from 1.5 to 30.2 cm and from 1.1 to 10.3 m, respectively (Table 1; Supplementary Figure S1c).

3.2 Allometric equation

We estimated the allometric equation between diameter of broken branch (*d* in cm) and its approximated volume (vbb in dm³) as:

TABLE 1 Measured characteristics of the 118 camphor trees and the 170 broken branches with range, mean and standard deviation (SD) of each characteristic, together with classes for the tree top status and for the broken branch diameter.

Characteristic	Range/class	Mean	SD
DBH (cm)	14.8–57.7	29.8	9.7
h_0 (height before the sleet) (m)	8.1–23.2	15.1	3.3
h_b (bole height) (m)	3.0–8.0	5.4	1.1
cd (crown diameter) (m)	3.2–17.5	8.1	3.5
h_1 (height after the sleet) (m)	6.3–18.2	11.0	2.4
Top status (0 for intact and 1 for broken top after the sleet)	0: 32; 1: 86	–	–
Number of broken branches	1–21	6.4	3.9
<i>d</i> (diameter of the broken branch) (cm)	1.5–30.2	5.5	3.8
<i>l</i> (length of the broken branch) (m)	1.1–10.3	3.9	1.8
dc (diameter class of broken branch) (interval in cm)	1–2: 13; 2–3: 93; 3–4: 72 4–5: 92; 5–6: 80; 6–7: 82 7–8: 64; 8–9: 48; 9–10: 7 10–11: 24; 11–12: 7; 12–13: 5 13–14: 0; 14–15: 2; 15–16: 1 16–17: 0; 17–18: 0; 18–19: 1	–	–
Number of twigs on the broken branch	2–13	4.5	2.0

$$vbb = e^{-3.325+2.611 \cdot \ln(d)} \quad (8)$$

The R^2 of this equation was 0.969 (Figure 3). Based on Equation 8, we estimated the volume of each diameter class (dc) of broken branches from 0.104 to 73.28 dm³ for dc from 1 to 18 cm.

3.3 Sleet damage

There were 86 out of the 118 (72.9%) camphor trees with broken tops (Table 1). The total volume of broken branches of each tree (vbtt) ranged from 0.39 to 375.34 dm³ with a mean of 70.40 dm³ and a standard deviation of 78.36 dm³ (Figure 4). With a Pearson's correlation coefficient of 0.93, vbtt was linearly correlated with the volume of broken stem (vs_b) ($p < 0.001$; Figure 4). Positive linear correlation was also identified between vbtt and the volume of broken crown (vc_b) (Pearson's correlation coefficient = 0.87, $p < 0.001$; Figure 4). The ratio between the volume of broken branches and of the

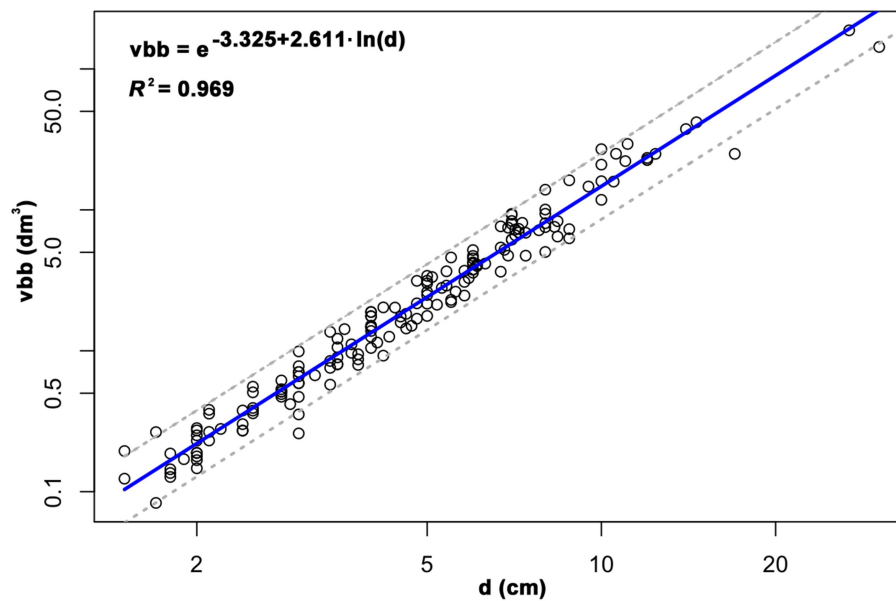


FIGURE 3

Scatterplot between diameter of broken branch (d ; cm) and estimated volume (vbb ; dm^3). The estimated allometric equation is $vbb = e^{-3.325+2.611 \cdot \ln(d)}$. p -values of the two estimated coefficients are both <0.001 , and R^2 of the equation is 0.969. The scatterplot uses the log–log scale, and the estimated equation is shown by the blue line with 95% prediction interval by the grey dotted lines.

stem before the sleet event ($rvbs$) was between 0.00068 and 0.39495 with a mean of 0.09492 and a standard deviation of 0.07813 (Figure 4).

3.4 Damage models

Our random forest regression models for $vbbt$, vs_b , vc_b , and $rvbs$ explained 54.0, 48.8, 61.2, and 12.2% of the variation, respectively, each with DBH, h_0 , cd , and h_b as explanatory variables (see variance importance plots of each model; Figures 5a,b for $vbbt$, Supplementary Figure S2 for ts , vs_b , vc_b , and $rvbs$). For ts , our random forest model had an error rate of 21.2% with 14.4% false positives and 6.8% false negatives, and its AUC was 0.72 (Supplementary Figure S3a).

Partial dependence plots of $vbbt$ on h_0 (Figure 5c), DBH (Figure 5d), cd (Figure 5e), h_b (Figure 5f), and combination of DBH and h_b (Figure 6) together with partial dependence plots of vs_b (Supplementary Figure S3b), vc_b (Supplementary Figure S3c), and $rvbs$ (Supplementary Figure S3d) in combination with DBH and h_b showed the marginal effects of DBH and h_b on the damage variables (i.e., $vbbt$, vs_b , vc_b , and $rvbs$, respectively). Larger $vbbt$ (Figure 6), vs_b (Supplementary Figure S3b) and vc_b (Figure 3c) were identified for trees with larger DBH and intermediate h_b , while higher $rvbs$ was only found in small trees with extremely small or large h_b (Supplementary Figure S3d).

Based on the partial dependence of $vbbt$ on DBH (Figure 5d), we estimated the volume of broken branches ($vbbt$) of a camphor tree with 35.0 cm DBH and with average height, crown diameter and bole height as 106.4 dm^3 . By multiplying this volume by camphor wood density, 0.52 kg/dm^3 (Miles and Smith, 2009; McPherson et al., 2016b), we estimated biomass loss from broken branches of this tree as 55.3 kg.

Two-way ANOVA and multiple comparison between each level of DBH and h_b on $vbbt$ confirmed that the camphor trees with DBH

above 40 cm and intermediate bole height (4.5–6.5 m) suffered significantly more damage in $vbbt$ than those with DBH below 27 cm and those between 27 and 40 cm regardless of bole height (TukeyHSD p -value <0.05 for each pair compared). However, for trees with DBH above 40 cm and larger bole height (above 6.5 m), no significant difference in damage as $vbbt$ was found comparing against trees at other levels of DBH regardless of bole heights ($p > 0.05$). Meanwhile, the camphor trees with bole height below 4.5 m suffered significantly less in terms of $vbbt$ from the sleet event than those with bole height between 4.5 and 5.5 m ($p = 0.03$). No significant difference in $vbbt$ was found in other pairs of comparison by levels of DBH or bole height of the camphor trees ($p > 0.05$).

4 Discussion

4.1 Sleet damage

Sleet damage to camphor trees can be estimated by tree size characteristics measured before the sleet event (i.e., DBH, height (h_0), crown diameter (cd), and bole height (h_b)). Based on the allometric relationship we built between diameter (d) and volume (vbb) of broken branches ($R^2 = 0.969$; Figure 3), we assessed sleet damage to street camphor trees in Wuhan, a mega-city in central China. Our random forest regression models explained 54.0, 48.8, and 61.2% of the variation for sleet damage to branches, stems, and crowns, respectively. DBH was the most important variable for estimating sleet damage to stems (Supplementary Figures S2c,d) and crowns (Supplementary Figures S2e,f). Broken tops are prevalent among street camphor trees at the rate of 72.9% (Table 1), which was predicted at an error rate of 21.2% by tree size characteristics (Supplementary Figure S3a). Overall, larger trees are expected to lose a greater volume of branches (Figure 6), stem

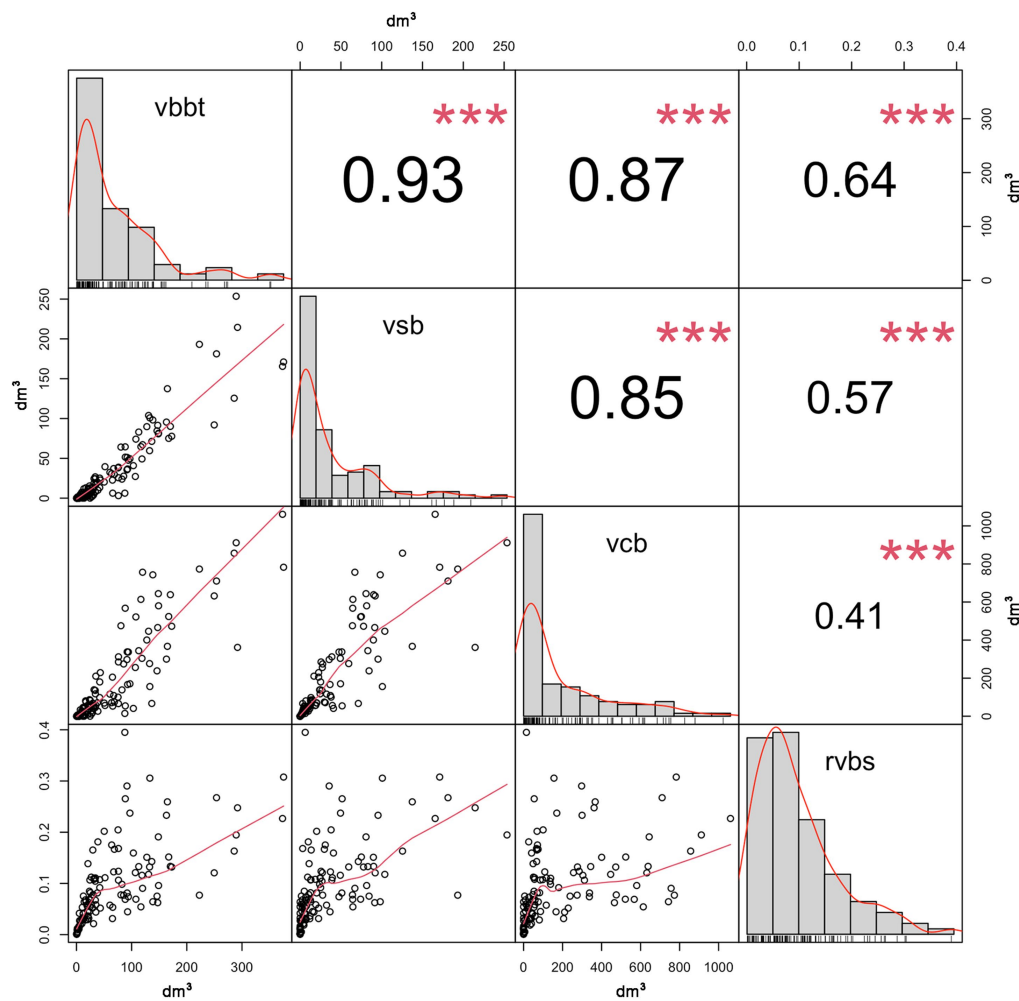


FIGURE 4

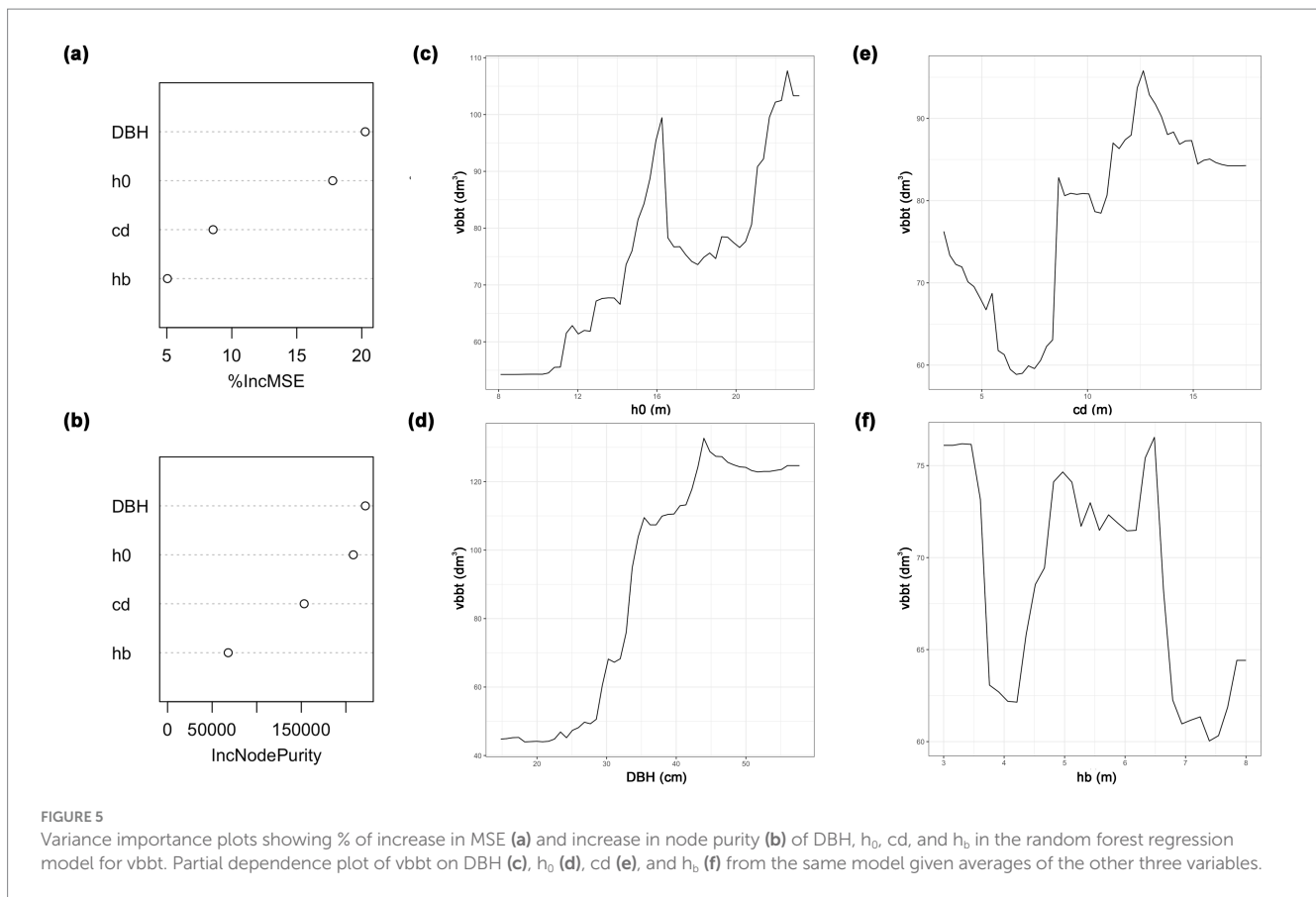
Distribution of the four continuous variables of sleet damage to branches (vbbt; dm^3), stems (vsb; dm^3), crowns (vcb; dm^3), and ratio between the volume of broken branches and of the stem before the sleet event (rvbs), together with scatterplots between each pair. Pearson's correlation coefficients between each pair is given with p -values (***) for $p < 0.001$). Distribution density of each variable and locally estimated scatterplot smoothing (LOESS) of each pair of variables are in red curves in histograms and scatterplots, respectively.

(Supplementary Figure S3b), and crown (Supplementary Figure S3c). Particularly, large trees with intermediate bole height (h_b) around 5.0 m are likely to suffer most from the sleet event (Figure 6; Supplementary Figures S3b,c). Two-way ANOVA and multiple comparison confirmed what we identified from the random forest regression models.

The ratio between the volume of broken branches and of the stem before the sleet event (rvbs) varied highly from 0.00068 to 0.39495. The mean ratio between the volume of broken branches and of the stem before the sleet event (rvbs) of 9.49% from the 118 street camphor trees was comparable to Zhao et al.'s (2020) estimated average loss of branch biomass due to a record-breaking ice storm event in 2008 for broadleaf evergreen trees ($9.0\% \pm 0.43\%$). We identified that trees with shorter bole height were expected to lose a higher ratio of their stem volume by the sleet event (Supplementary Figure S3d), though the random forest regression model explained only 12.2% of variation in rvbs. We estimated that camphor trees with DBH larger than 18 cm would lose between 5 and 15% of their stem volumes, and those with bole height larger than

3.7 m suffered less (Supplementary Figure S3d). Previous studies found similar patterns of snow damage to trees in a temperate secondary forest in northeast China (Li et al., 2018), a subtropical forest transect across southern China (Shao et al., 2011), and a national forest farm in southern China (Zhao et al., 2020), which implied that larger trees (i.e., taller trees and trees with wider crowns) tend to break more due to weight accumulated from snow but the percentage of volume lost was similar to smaller trees (Shao et al., 2011; Li et al., 2018; Gao et al., 2024).

The record-breaking sleet event (Figure 1b) caused branch, stem, and crown damage to over 100 thousand camphor trees planted in Wuhan (Wuhan Municipal Landscape Gardens and Forestry Bureau, 2024), and more in central China (Xiang et al., 2020). The severity of damage caused by the sleet event was unusually high as no camphor tree measured in this study had intact branches, which was higher than the damage by the 2008 ice storm event to trees in southern China (Zhao et al., 2020). Monitoring studies showed that the structure and functions of the damaged forests was not yet fully recovered 15 years after the ice storm event (Gao et al., 2024). Recovery of the impacted



street camphor trees in central China could be costly as they require clearing, pruning, and nourishing to regain their health and places in the urban ecosystem (McPherson et al., 2016a; Yan and Yang, 2018; Chau et al., 2020; Liu and Slik, 2022). Municipal councils need to consider ecological functional benefits, structural values, and costs of maintaining damaged street trees to decide where to invest their management efforts to recover from sleet damage (Wang et al., 2018).

4.2 Implications

Tree size and shape have been found to be significant for predicting sleet (DBH and bole height in this study) and snow damage (Hauer et al., 1993; Yan and Yang, 2018; Tavankar et al., 2019). Based on the partial dependence plots of DBH and bole height (h_b) derived from the random forest regression models for vbbt (Figure 6), vs_b (Supplementary Figure S3b), and vc_b (Supplementary Figure S3c), we suggest that pruning, instead of topping the main stems of camphor trees, as a way to elevate bole height (Zhou and Yan, 2016; Speak and Salbitano, 2023), might be practical for reducing future heavy sleet damage to camphor trees. Studies on the effect of pruning on damage reduction support our finding and suggestion (Bragg et al., 2003; Levia et al., 2017; Li et al., 2018; Wang et al., 2018; Poni et al., 2022). Pruning before winter reduces the stress of weight added to branches and enhances tree resilience to ice and snow damage (Bragg et al., 2003; Levia et al., 2017; Li et al., 2018). Pruning is also a regular practice to prevent frost damage to trees (Poni et al., 2022). Snow damage to crowns was found to be related to crown topographical conditions (Tavankar

et al., 2019), which might also be managed by pruning (McPherson et al., 2016b). It is also notable that the resistance of street trees to disturbances is affected by both climate conditions and management practices such as topping, nursery, and pruning (Yang et al., 2012).

Pruning street trees is costly, but it becomes economic when considering the cost of labor for clearing broken branches and the amount of carbon released from broken branches (Velázquez-Martí et al., 2011; Wang et al., 2018). Clearing broken branches of these many camphor trees required much labor and an unexpected cost for street tree maintenance (Wang et al., 2018). This would limit the amount of care, such as pruning and pest prevention (Xiang et al., 2020; Speak and Salbitano, 2023), on street trees, further decreasing their resistance to natural disasters and pests. Moreover, broken branches were collected and treated as residual waste by city cleaners, so their biomass would be released to atmosphere as a carbon source, which were reported to contribute to carbon emissions in major cities of China (Shi et al., 2013). We estimated that, on average, a street camphor tree with 35.0 cm DBH lost 55.3 kg biomass in branches damaged by the sleet event. Considering that camphor trees account for near 10% of street trees in Wuhan (Tian et al., 2024), the net carbon loss from biomass in branches damaged by the sleet event might be a source of carbon in millions of kg (Yan and Yang, 2018).

4.3 Limitations

The damage was by far the heaviest sleet damage on record in Wuhan (Weather Station of Wuhan, 2024), and it was the first sleet

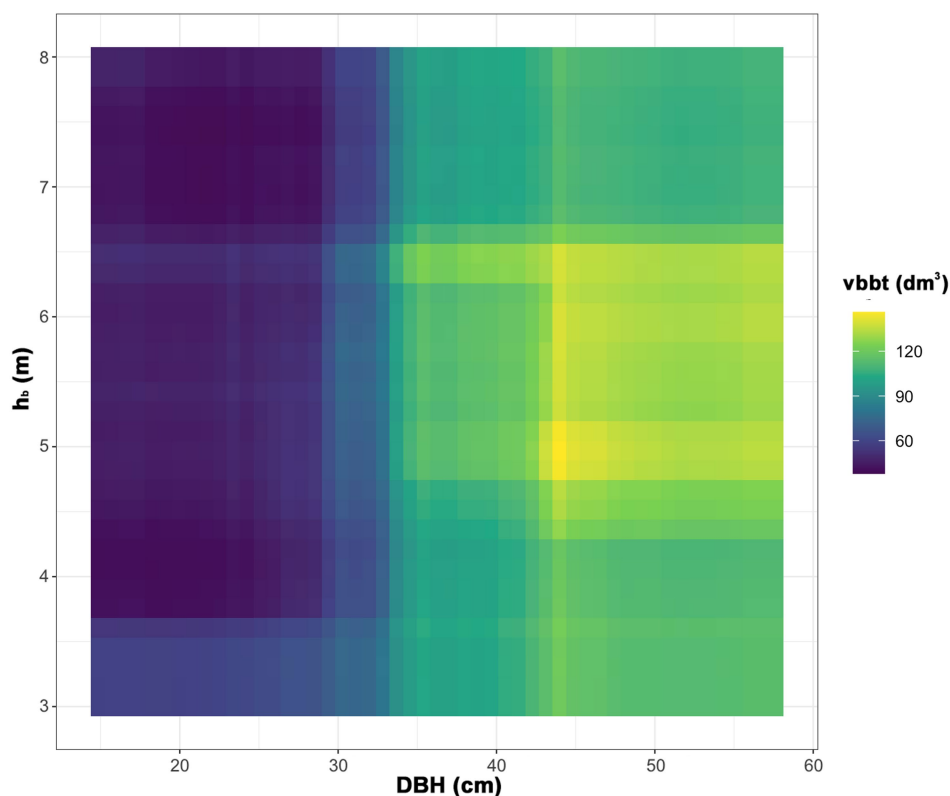


FIGURE 6
Partial dependence plot of total volume of broken branches (vbbt; dm^3) on DBH (cm) and h_b (m) given average height (h_0) and crown diameter (cd) derived from the random forest regression model for vbbt with DBH, h_0 , cd, and h_b as explanatory variables.

event in the winter of 2023–2024 (Figure 1b). Sleet damage to camphor trees would likely vary if the strength and frequency of future sleet events and its accompanying weather conditions, such as temperature and wind, differ from this event (Zhu et al., 2004; Gao et al., 2024). It may also be different if level of urban development (Tian et al., 2024), topographical conditions (Tavankar et al., 2019), and tree characteristics (Yang et al., 2023) differ from street camphor trees growing in our study area. Damage due to any addition to the layer of frozen water at the surfaces of leaves and branches after the sleet event could confound damage due to the sleet event (Livanov, 2023), but this bias was minor in our study because the temperature increased to above 0°C two days after the end of the sleet event (Figure 1b) and because damage assessment was completed before the temperature decreased below 0°C . This reduced any bias due to damage by other weather events. Models for estimating sleet damage might be improved if tree shape and size characteristics other than DBH, height and crown diameter were measured and included (Proulx and Greene, 2001; Niinemets, 2016; Zhao et al., 2020). However, measuring these variables requires additional time and labor. Our random forest regression models for sleet damage to branches, stems, and crowns were useful for understanding how sleet damage were related to DBH and bole height (Figure 6; Supplementary Figures S3b,c), two important size and shape characters of street camphor trees. We argue that the models built in this study can be used for assessing damage to other street camphor trees in Wuhan by the same record-breaking sleet event (from 2nd to

4th February 2024; Figure 1b), but the models should be refitted if future sleet events occurred under different weather conditions. Levels of sleet damage to camphor trees are subject to the strength of sleet events, including duration, precipitation, vapor pressure, and the rate of temperature change (Gay and Davis, 1993; Livanov, 2023). This study specifically modelled the first sleet event in the winter of 2023–2024, which was also the most severe sleet event that winter (Weather Station of Wuhan, 2024). Camphor trees continued to experience damage by cold weather events after the sleet event, but the degree of damage was much less severe because branches vulnerable to the formation of heavy ice layers were already broken in the initial sleet event (Zhao et al., 2020; Gao et al., 2024) and because subsequent cold weather events were less severe (Weather Station of Wuhan, 2024). We therefore did not plan to survey damage to camphor trees caused by subsequent cold weather events in Wuhan, but it would be necessary to conduct consecutive damage monitoring on the same group of trees to assess the impacts of cold weather events on branches of camphor trees for different levels of severity in future studies.

Stem and crown volume could be more accurately measured using a laser scanner (Chianucci et al., 2020), although we approximated them for damage assessment by balancing measurement accuracy and model performance (Bornand et al., 2023). Constrained by labor, the sizes of broken branches were not completely measured. However, we managed to count and class diameters (dc) of all broken branches with $d \geq 1$ cm on the main stem due to sleet, and established the allometric equation between diameter (d) and volume (vbb) of broken

branches based on measured data. Allometric equations with different forms have been used in other studies (Bornand et al., 2023), but our equation had a simple format and a high R^2 (i.e., 0.969). Our equation also had the same format as previously established equations for camphor trees (Pillsbury et al., 1998) and other street tree species in China (Yang et al., 2023). For parsimony and based on previous studies, we chose to use this allometric equation to estimate the volume for each dc. Twigs on broken branches were not included in this study, which would lead to an underestimation of sleet damage. To account for missing twigs, we also excluded branch volume in the denominator of rvbs. It is worth mentioning that this allometric equation might be less accurate if used for camphor trees growing in other areas with different environmental conditions (Xu et al., 2021; Guo et al., 2024). We did no extrapolation of the allometric equation or the random forest regression models in this study, which should be done with caution for trees of different sizes to be measured and modelled.

4.4 Future research

Under climate change, extreme weather events became emerging concerns as their negative impacts on ecosystems and humans grow too large, both regionally and locally, to be ignored (Stott, 2016; Ummenhofer and Meehl, 2017). Particularly in recent years, for instance in 2023, persistent and large-scale hot-dry weather drove extremely large forest fires in Canada, releasing 647 Tg carbon emissions, comparable to India's annual emissions (Byrne et al., 2024). Locally, areas experiencing elongated freezing days have been expanding rapidly, and the levels and uncertainty of damage due to extreme cold weathers have been increasing (Ummenhofer and Meehl, 2017). Studies on the impacts of extreme weather events, especially those less common in the past decades in certain areas, such as sleet events in central China (Lv et al., 2011), need to be conducted on the main tree species for improved understanding of damage due to these extreme weather events and for preparing for future extreme weathers.

As sleet events become more frequent and severe under climate change in areas populated with evergreen trees (Ohba, 2021), studies on sleet damage to other dominant street trees, such as *Ligustrum lucidum* and *Magnolia grandiflora* (Xiang et al., 2020), and on trees growing in plantations and forests are needed to fully assess sleet damage to trees and the global carbon cycle (Tavankar et al., 2019; Braghiroli and Passarini, 2020), as well as for mitigating the negative impacts of climate change. For street camphor trees, how much pruning and at what point in the trees' life cycles it should be carried out to minimize future sleet damage need to be further tested (Hauer et al., 1993; Campos et al., 2023). Apart from pruning, spacing and planting stands mixed with deciduous trees might help reduce sleet damage to camphor trees (Li et al., 2018; Chau et al., 2020). Breeding for tall trees and trees with short bole height might be helpful for them to survive sleet events (Yang et al., 2023). Specific management strategies for conserving damaged camphor trees of different ecological functional values need to be fully discussed (Wang et al., 2018). Additionally, street camphor trees growing in other major cities in China may develop different allometries and suffer differently from extreme weather events (Tian et al., 2024), which should be further

studied to understand how to conserve street camphor trees across different climate zones. The methods from this study may be applied to help answer these questions, and model damage by other extreme weather events, such as ice storm and heavy snow, which are expected to occur more frequently under climate change (Rummukainen, 2012).

5 Conclusion

The record-breaking sleet event in Wuhan damaged street camphor trees disproportionately by their size with a mean height decrease of 4.3 m. Larger camphor trees with DBH above 40 cm were found to suffer more from the sleet event, and trees with intermediate bole height between 4.5 and 6.5 m were found to suffer more damage. There was an allometric relationship between diameter and volume of broken branches of camphor trees. On average, a street camphor tree with 35.0 cm DBH was estimated to lose 106.4 dm³ branches (equivalent to 55.3 kg biomass) from the sleet event. Pruning periodically to control bole height before sleet events would be helpful to reduce future heavy sleet damage. As sleet and other extreme weather events become more frequent and severe under climate change, it is necessary to test the effect of pruning to street trees and to model damage by the extreme weather events on different tree species, especially evergreen broadleaf tree species, to mitigate the negative impacts of climate change on street trees and urban forest ecosystems.

Data availability statement

The raw data supporting the conclusions of this article will be made available by the authors, without undue reservation.

Author contributions

YL: Writing – original draft, Data curation, Investigation, Methodology, Validation. JZ: Data curation, Resources, Validation, Writing – original draft, Project administration. SR: Data curation, Formal analysis, Visualization, Writing – original draft. KX: Conceptualization, Formal analysis, Funding acquisition, Investigation, Methodology, Project administration, Supervision, Validation, Writing – original draft, Writing – review & editing.

Funding

The author(s) declare that financial support was received for the research, authorship, and/or publication of this article. The work was supported by the Hubei Province Young Science and Technology Talent Morning Light Lift Project, Hubei Association for Science and Technology, Wuhan, China [grant number 202344].

Acknowledgments

We thank Feiling Liu for field survey in the cold winter.

Conflict of interest

The authors declare that the research was conducted in the absence of any commercial or financial relationships that could be construed as a potential conflict of interest.

Publisher's note

All claims expressed in this article are solely those of the authors and do not necessarily represent those of their affiliated

organizations, or those of the publisher, the editors and the reviewers. Any product that may be evaluated in this article, or claim that may be made by its manufacturer, is not guaranteed or endorsed by the publisher.

Supplementary material

The Supplementary material for this article can be found online at: <https://www.frontiersin.org/articles/10.3389/ffgc.2024.1391645/full#supplementary-material>

References

- Bornand, A., Rehus, N., Morsdorf, F., Thürig, E., and Abegg, M. (2023). Individual tree volume estimation with terrestrial laser scanning: evaluating reconstructive and allometric approaches. *Agric. For. Meteorol.* 341:109654. doi: 10.1016/j.agrformet.2023.109654
- Bragg, D. C., Shelton, M. G., and Zeide, B. (2003). Impacts and management implications of ice storms on forests in the southern United States. *For. Ecol. Manag.* 186, 99–123. doi: 10.1016/S0378-1127(03)00230-5
- Braghiroli, F. L., and Passarini, L. (2020). Valorization of biomass residues from forest operations and wood manufacturing presents a wide range of sustainable and innovative possibilities. *Curr. For. Rep.* 6, 172–183. doi: 10.1007/s40725-020-00112-9
- Breiman, L. (2001). Random forests. *Mach. Learn.* 45, 5–32. doi: 10.1023/A:1010933404324
- Burke, M. J., Gusta, L. V., Quamme, H. A., Weiser, C. J., and Li, P. H. (1976). Freezing and injury in plants. *Annu. Rev. Plant Physiol.* 27, 507–528. doi: 10.1146/annurev.pp.27.060176.002451
- Byrne, B., Liu, J., Bowman, K. W., Pascolini-Campbell, M., Chatterjee, A., Pandey, S., et al. (2024). Carbon emissions from the 2023 Canadian wildfires. *Nature* 633, 835–839. doi: 10.1038/s41586-024-07878-z
- Campos, R., Harvey, P. S., and Hou, G. (2023). Analytical fragility curves for trees subject to ice loading in a changing climate. *Sustain. Resilient Infrastruct.* 8, 555–571. doi: 10.1080/23789689.2023.2202962
- Carl, P., Peterson, B. G., and Peterson, M. B. G. (2010). Package 'PerformanceAnalytics'. Available at: <https://cran.r-project.org/web/packages/PerformanceAnalytics/PerformanceAnalytics.pdf> (accessed February 14, 2024).
- Chau, N. L., Jim, C. Y., and Zhang, H. (2020). Species-specific holistic assessment of tree structure and defects in urban Hong Kong. *Urban For. Urban Green.* 55:126813. doi: 10.1016/j.ufug.2020.126813
- Chen, J., Tang, C., Zhang, R., Ye, S., Zhao, Z., Huang, Y., et al. (2020). Metabolomics analysis to evaluate the antibacterial activity of the essential oil from the leaves of *Cinnamomum camphora* (Linn.) Presl. *J. Ethnopharmacol.* 253:112652. doi: 10.1016/j.jep.2020.112652
- Chianucci, F., Puletti, N., Grotti, M., Ferrara, C., Giorcelli, A., Coaloa, D., et al. (2020). Nondestructive tree stem and crown volume allometry in hybrid poplar plantations derived from terrestrial laser scanning. *For. Sci.* 66, 737–746. doi: 10.1093/forsci/fxaa021
- Chupp, A. D., and Battaglia, L. L. (2016). Bird-plant interactions and vulnerability to biological invasions. *J. Plant Ecol.* 9, 692–702. doi: 10.1093/jpe/rtw020
- Downton, M. W., and Miller, K. A. (1993). The freeze risk to Florida citrus. Part II: temperature variability and circulation patterns. *J. Clim.* 6, 364–372. doi: 10.1175/1520-0442(1993)006<0364:TFRTFC>2.0.CO;2
- Gao, G., Li, Z., and Zhou, B. (2024). "Impact of the 2008 ice storm on forests in Southeast China" in *The handbook of environmental chemistry*. eds. Y. Wang, M. E. Lucas Borja, Z. Sun and P. Pereira (Berlin, Heidelberg: Springer), 1–27.
- Garg, A., and Tai, K. (2013). Comparison of statistical and machine learning methods in modelling of data with multicollinearity. *Int. J. Model. Identif. Control.* 18, 295–312. doi: 10.1504/IJMIC.2013.053535
- Gay, D. A., and Davis, R. E. (1993). Freezing rain and sleet climatology of the southeastern USA. *Clim. Res.* 3, 209–220. doi: 10.3354/cr003209
- Gómez, F., Jabaloyes, J., Montero, L., De Vicente, V., and Valcuende, M. (2011). Green areas, the most significant indicator of the sustainability of cities: research on their utility for urban planning. *J. Urban Plan. Dev.* 137, 311–328. doi: 10.1061/(ASCE)UP.1943-5444.0000060
- Greenwell, B. M. (2017). Pdp: an R package for constructing partial dependence plots. *R J* 9, 421–436. doi: 10.32614/RJ-2017-016
- Guo, C., Hu, Y., Qin, J., Wu, D., Xu, L., and Wang, H. (2024). Comparison of crown volume increment in street trees among six cities in western countries and China. *Horticulturae* 10:300. doi: 10.3390/horticulturae10030300
- Hauer, R. J., Wang, W., and Dawson, J. O. (1993). Ice storm damage to urban trees. *J. Arboric.* 19, 187–194. doi: 10.48044/jauf.1993.031
- Ireland, L. C. (2000). Ice storms and forest impacts. *Sci. Total Environ.* 262, 231–242. doi: 10.1016/S0048-9697(00)00525-8
- Jucker, T., Fischer, F. J., Chave, J., Coomes, D. A., Caspersen, J., Ali, A., et al. (2022). Tallo: a global tree allometry and crown architecture database. *Glob. Change Biol.* 28, 5254–5268. doi: 10.1111/gcb.16302
- Karl, T. R., Meehl, G. A., Miller, C. D., Hassol, S. J., Waple, A. M., and Murray, W. L. (2008). Weather and climate extremes in a changing climate. Washington, D.C., USA: NOAA National Climatic Data Center.
- Levia, D. F., Hudson, S. A., Llorens, P., and Nanko, K. (2017). Throughfall drop size distributions: a review and prospectus for future research. *WIREs Water* 4:e1225. doi: 10.1002/wat2.1225
- Li, X., Jin, L., Zhu, J., Liu, L., Zhang, J., Wang, Y., et al. (2018). Response of species and stand types to snow/wind damage in a temperate secondary forest, Northeast China. *J. For. Res.* 29, 395–404. doi: 10.1007/s11676-017-0446-z
- Liang, C., Jiang, H., Yang, S., Tian, P., Ma, X., Tang, Z., et al. (2024). Characterizing street trees in three metropolises of central China by using street view data: from individual trees to landscape mapping. *Ecol. Inform.* 80:102480. doi: 10.1016/j.ecoinf.2024.102480
- Liu, J., and Slik, F. (2022). Are street trees friendly to biodiversity? *Landsc. Urban Plan.* 185:104304. doi: 10.1016/j.landurbplan.2021.104304
- Livanov, D. (2023). "The weather and climate" in *The physics of planet earth and its natural wonders*. eds. E. Yamburg and A. Furchenko (Springer Nature, Switzerland: Cham), 241–297.
- Lv, J., Wu, H., and Chen, M. (2011). Effects of nitrogen and phosphorus on phytoplankton composition and biomass in 15 subtropical, urban shallow lakes in Wuhan, China. *Limnologia* 41, 48–56. doi: 10.1016/j.limno.2010.03.003
- Matsushita, A. K., Gonzalez, D., Wang, M., Doan, J., Qiao, Y., and McKittrick, J. (2020). Beyond density: mesostructural features of impact resistant wood. *Mater. Today Commun.* 22:100697. doi: 10.1016/j.mtcomm.2019.100697
- Maxwell, S. L., Butt, N., Maron, M., McAlpine, C. A., Chapman, S., Ullmann, A., et al. (2019). Conservation implications of ecological responses to extreme weather and climate events. *Divers. Distrib.* 25, 613–625. doi: 10.1111/ddi.12878
- McPherson, E. G., van Doorn, N. S., and de Goede, J. (2016a). Structure, function and value of street trees in California, USA. *Urban For. Urban Green.* 17, 104–115. doi: 10.1016/j.ufug.2016.03.013
- McPherson, E. G., van Doorn, N. S., and Peper, P. J. (2016b). Urban tree database and allometric equations. Gen. Tech. Rep. PSW-GTR-23. Albany, CA, USA: US Department of Agriculture, Forest Service, Pacific Southwest Research Station, 86.
- Miles, P. D., and Smith, W. B. (2009). Specific gravity and other properties of wood and bark for 156 tree species found in North America. Res. Note NRS-38. Newtown Square, PA, USA: US Department of Agriculture, Forest Service, Northern Research Station, 35.
- Mohler, C. L., Marks, P. L., and Sprugel, D. G. (1978). Stand structure and allometry of trees during self-thinning of pure stands. *J. Ecol.* 66, 599–614. doi: 10.2307/2259153
- Niinemetts, Ü. (2016). Does the touch of cold make evergreen leaves tougher? *Tree Physiol.* 36, 267–272. doi: 10.1093/treephys/tpw007
- Ohba, M. (2021). "Precipitation under climate change" in *Precipitation*. ed. J. Rodrigo-Comino (Amsterdam: Elsevier), 21–51.
- Pillsbury, N. H., Reimer, J. L., and Thompson, R. P. (1998). Tree volume equations for fifteen urban species in California. Tech. Rep. 7. San Luis Obispo, CA: Urban Forest Ecosystems Institute, California Polytechnic State University, 56.
- Poni, S., Sabbatini, P., and Palliotti, A. (2022). Facing spring frost damage in grapevine: recent developments and the role of delayed winter pruning—a review. *Am. J. Enol. Vitic.* 73, 211–226. doi: 10.5344/ajev.2022.22011

- Proulx, O. J., and Greene, D. F. (2001). The relationship between ice thickness and northern hardwood tree damage during ice storms. *Can. J. For. Res.* 31, 1758–1767. doi: 10.1139/x01-104
- R Core Team (2023). R: A language and environment for statistical computing. Vienna, Austria: R Foundation for Statistical Computing.
- Rummukainen, M. (2012). Changes in climate and weather extremes in the 21st century. *WIREs Clim. Change* 3, 115–129. doi: 10.1002/wcc.160
- Shao, Q., Huang, L., Liu, J., Kuang, W., and Li, J. (2011). Analysis of forest damage caused by the snow and ice chaos along a transect across southern China in spring 2008. *J. Geogr. Sci.* 21, 219–234. doi: 10.1007/s11442-011-0840-y
- Shi, Y., Ge, Y., Chang, J., Shao, H., and Tang, Y. (2013). Garden waste biomass for renewable and sustainable energy production in China: potential, challenges and development. *Renew. Sust. Energ. Rev.* 22, 432–437. doi: 10.1016/j.rser.2013.02.003
- Speak, A. F., and Salbitano, F. (2023). The impact of pruning and mortality on urban tree canopy volume. *Urban For. Urban Green.* 79:127810. doi: 10.1016/j.ufug.2022.127810
- Stereńczak, K., Mielcarek, M., Wertz, B., Bronisz, K., Zajączkowski, G., Jagodziński, A. M., et al. (2019). Factors influencing the accuracy of ground-based tree-height measurements for major European tree species. *J. Environ. Manag.* 231, 1284–1292. doi: 10.1016/j.jenvman.2018.09.100
- Stott, P. (2016). How climate change affects extreme weather events. *Science* 352, 1517–1518. doi: 10.1126/science.aaf7271
- Tavankar, F., Lo Monaco, A., Nikooy, M., Venanzi, R., Bonyad, A., and Picchio, R. (2019). Snow damages on trees of an uneven age in mixed broadleaf forests: effects of topographical conditions and tree characteristics. *J. For. Res.* 30, 1383–1394. doi: 10.1007/s11676-018-0710-x
- Tian, P., Liang, C., Zhang, J., Xiao, L., Wang, K., Yang, Y., et al. (2024). Geo-climates and street developments shape urban tree characteristics: a street-view inventory analysis of over 200,000 trees of 11 metropolises in China. *Sci. Total Environ.* 912:169503. doi: 10.1016/j.scitotenv.2023.169503
- Turcotte, M. M., Corrin, M. S., and Johnson, M. T. (2012). Adaptive evolution in ecological communities. *PLoS Biol.* 10:e1001332. doi: 10.1371/journal.pbio.1001332
- Ummenhofer, C. C., and Meehl, G. A. (2017). Extreme weather and climate events with ecological relevance: a review. *Philos. Trans. R. Soc. B* 372:20160135. doi: 10.1098/rstb.2016.0135
- Velázquez-Martí, B., Fernández-González, E., López-Cortés, I., and Salazar-Hernández, D. M. (2011). Quantification of the residual biomass obtained from pruning of trees in Mediterranean olive groves. *Biomass Bioenergy* 35, 3208–3217. doi: 10.1016/j.biombioe.2011.04.042
- Wang, X., Huang, S., Li, J., Zhou, G., and Shi, L. (2016). Sprouting response of an evergreen broad-leaved forest to a 2008 winter storm in Nanling Mountains, southern China. *Ecosphere* 7:e01395. doi: 10.1002/ecs2.1395
- Wang, Y. P., and Jarvis, P. G. (1990). Influence of crown structural properties on PAR absorption, photosynthesis, and transpiration in Sitka spruce: application of a model (MAESTRO). *Tree Physiol.* 7, 297–316. doi: 10.1093/treephys/7.1-2-3-4.297
- Wang, X., Yao, J., Yu, S., Miao, C., Chen, W., and He, X. (2018). Street trees in a Chinese forest city: structure, benefits and costs. *Sustain. For.* 10:674. doi: 10.3390/su10030674
- Weather Station of Wuhan. (2024). *Hubei ups emergency response to rain, snowstorms*. Available at: https://english.wuhan.gov.cn/H_1/NWP/202402/t20240223_2362765.shtml (Accessed February 28, 2024).
- White, J. (1981). The allometric interpretation of the self-thinning rule. *J. Theor. Biol.* 89, 475–500. doi: 10.1016/0022-5193(81)90363-5
- Wood, E. M., and Esaian, S. (2020). The importance of street trees to urban avifauna. *Ecol. Appl.* 30:e02149. doi: 10.1002/eap.2149
- Wu, J. (2019). Developing general equations for urban tree biomass estimation with high-resolution satellite imagery. *Sustain. For.* 11:4347. doi: 10.3390/su11164347
- Wu, C. C., Chang, S. H., Tung, C. W., Ho, C. K., Gogorcena, Y., and Chu, F. H. (2020). Identification of hybridization and introgression between *Cinnamomum kanehirae* Hayata and *C. camphora* (L.) Presl using genotyping-by-sequencing. *Sci. Rep.* 10:15995. doi: 10.1038/s41598-020-72775-0
- Wuhan Municipal Landscape Gardens and Forestry Bureau (2024) Why do camphor trees frequently break branches under ice and snow? Available at: https://ylj.wuhan.gov.cn/xwdt/mtbd_12295/202402/t20240206_2357790.shtml (accessed February 17, 2024).
- Xiang, Z., Zhao, M., and Ogbodo, U. S. (2020). Accumulation of urban insect pests in China: 50 years' observations on camphor tree (*Cinnamomum camphora*). *Sustain. For.* 12:1582. doi: 10.3390/su12041582
- Xiao, Y., Li, M., and Chen, F. (2023). Root rot of *Cinnamomum camphora* (Linn) Presl caused by *Phytophthora vexans* in China. *Plan. Theory* 12:1072. doi: 10.3390/plants12051072
- Xu, K., Jiang, J., and He, F. (2021). Climate-based allometric biomass equations for five major Canadian timber species. *Can. J. For. Res.* 51, 1633–1642. doi: 10.1139/cjfr-2020-0485
- Yan, P., and Yang, J. (2018). Performances of urban tree species under disturbances in 120 cities in China. *Forests* 9:50. doi: 10.3390/f9020050
- Yang, J., Zhang, M., Zhang, J., Lu, H., and Hauer, R. J. (2023). Allometric growth of common urban tree species in Qingdao City of eastern China. *Forests* 14:472. doi: 10.3390/f14030472
- Yang, J., Zhou, J., Ke, Y., and Xiao, J. (2012). Assessing the structure and stability of street trees in Lhasa, China. *Urban For. Urban Green.* 11, 432–438. doi: 10.1016/j.ufug.2012.07.002
- Zhang, J., Qu, X., Huang, Y., Tan, M., and Xu, K. (2024). Assessing the potential of species loss caused by deforestation in a mature subtropical broadleaf forest in Central China. *Trees For. People* 18:100673. doi: 10.1016/j.tfp.2024.100673
- Zhao, H., Li, Z., Zhou, G., Qiu, Z., and Wu, Z. (2020). Aboveground biomass allometric models for evergreen broad-leaved forest damaged by a serious ice storm in southern China. *Forests* 11:320. doi: 10.3390/f11030320
- Zhou, Y., and Yan, W. (2016). Conservation and applications of camphor tree (*Cinnamomum camphora*) in China: ethnobotany and genetic resources. *Genet. Resour. Crop. Evol.* 63, 1049–1061. doi: 10.1007/s10722-015-0300-0
- Zhu, J., Liu, Z., Li, X., Matsuzaki, T., and Gonda, Y. (2004). Review: effects of wind on trees. *J. For. Res.* 15, 153–160. doi: 10.1007/BF02856753